The Role of Clouds, Water Vapor, Circulation, and Boundary Layer Structure in the Sensitivity of the Tropical Climate

KRISTIN LARSON AND DENNIS L. HARTMANN

Department of Atmospheric Sciences, University of Washington, Seattle, Washington

STEPHEN A. KLEIN

NOAA/Geophysical Fluid Dynamics Laboratory, Princeton University, Princeton, New Jersey

ABSTRACT

The physical mechanisms that affect the tropical sea surface temperature (SST) are investigated using a two-box equilibrium model of the Tropics. One box represents the convecting, warm SST, high humidity region of the Tropics, and the other box represents the subsidence region with low humidity, boundary layer clouds, and cooler SST. The two regions communicate by energy and moisture fluxes that are proportional to the strength of the overturning circulation that couples the two regions. The boundary layer properties in the subsiding region are predicted with a mixing line model. Humidity above the inversion in the subsiding region is predicted from moisture conservation.

The humidity above the inversion in the subsiding region increases rapidly with temperature, but this has less effect on the sensitivity than expected, because the inversion lowers as the humidity above the inversion is increased. Some of the increased greenhouse effect of the free troposphere can be offset by decreased greenhouse effect of the boundary layer. Increasing the area of the warm, convective region increases the SSTs, because of the greenhouse effect of the greater upper-tropospheric water vapor in the convective region. The circulation strength is constrained by radiative cooling in the cold pool. The strength of the circulation decreases with increasing convective area, because the increase in dry static stability overwhelms the increase in cooling rate. Although they have strong individual effects on longwave and shortwave radiation, high clouds in the convective region do not affect the tropical SSTs strongly, because their net radiative forcing at the top of the atmosphere is small. Low clouds in the subsidence region have a strong cooling affect on the tropical SST, because they strongly reduce net radiative heating at the top of the atmosphere. A negative feedback is produced if the low clouds are predicted from the observed relationship between stratus cloud amount and lower-tropospheric stability.

1. Introduction

In recent years much effort has been expended in attempts to better understand the sensitivity of the tropical climate. At temperatures near those of warm waters of the tropical ocean, the absorption of longwave radiation by water vapor increases rapidly with temperature. As a result, longwave cooling of the surface actually decreases with increasing temperature (e.g., Raval and Ramanathan 1989; Hartmann 1994; Inamdar and Ramanathan 1994). Because this cooling may constitute a strong positive feedback for the surface energy budget, it is important to identify mechanisms that regulate the tropical surface temperature. Several approaches to understanding the apparent stability of tropical sea surface temperatures (SSTs) have recently appeared in the literature. Ramanathan and Collins (1991) proposed that the reflection of solar radiation by tropical convective clouds increases rapidly with surface temperature, so that the solar heating of the warm surface under the convective clouds decreases with increasing SST at a rate more than sufficient to offset the reduced longwave loss. Others have argued that large-scale dynamics causes the atmosphere above the warmest waters to communicate rapidly with the atmosphere above cooler water (e.g., Fu et al. 1992; Wallace 1992). Pierrehumbert (1995) argued that energy is transported from the humid convective regions of the Tropics to regions of subsidence, where high temperatures and low humidities provide efficient cooling to space. Cloud models suggest that large-scale convergence is more important than SSTs in generating high cloud albedos (Lau et al. 1994), and observations suggest that cloud radiative forcing is better correlated with large-scale divergence than with SST (e.g., Hartmann and Michelsen 1993). Because of

Corresponding author address: Ms. Kristin Larson, Department of Atmospheric Sciences, University of Washington, P.O. Box 351640, Seattle, WA 98195-1640.
E-mail: klarson@atmos.washington.edu

this dependence on large-scale circulation, changes in cloud albedo in regions where SSTs warm during ENSO events are offset by changes of opposite sign in adjacent regions (Hartmann and Michelsen 1993). If convection or large-scale motions act to keep the boundary layer air sufficiently dry, then evaporation can increase at a rate sufficient to offset the decreased longwave loss and keep the surface energy budget balanced at observed temperatures (e.g., Hartmann and Michelsen 1993). Ocean dynamics has also been suggested as a mechanism that can moderate tropical SSTs (Clement et al. 1996; Sun and Liu 1996). Miller (1997) proposed that the amount of low cloud cover in the nonconvective regions of the Tropics could be a strong negative feedback. Miller used an empirical relationship between lower-tropospheric stability (LTS) and stratus cloud amount from Klein and Hartmann (1993).

Many questions addressed by these studies about the tropical climate remain at issue. What effects do the Hadley and Walker circulations have on tropical climate change? How does the amount of convective cloud affect the tropical SST locally and in remote regions? How do stratus cloud decks in the subsidence region of the Tropics interact with the highly convective regions? How is the upper-tropospheric humidity in subsidence regions affected by changes in SST? What climate feedbacks are most important in the Tropics, and how will they affect the global climate when the amount of carbon dioxide is doubled?

These questions are investigated in this study using a two-box equilibrium energy and moisture balance model. In particular, the humidity above the inversion in the subsiding regions will be predicted and its role in climate sensitivity addressed. The simple model includes the interaction between a warm SST region where deep convection occurs (referred to as the warm pool) and another tropical region where the SST is slightly lower and convection is suppressed by large-scale subsidence (the cold pool). These regions are connected by heat and water vapor budgets, and temperature, humidity, and the mass circulation between the regions are predicted. Ocean fluxes, atmospheric heat export to the extratropics, surface wind speed, and cloud optical properties are all external parameters for the present implementation of the model. Unlike previous two-box models (Miller 1997; Pierrehumbert 1995; Clement and Seager 1999, manuscript submitted to *J. Climate*), the trade inversion height is determined by the model and the moisture in the upper troposphere of the cold pool is predicted.

We investigate the response of the equilibrium climate of this model to the radiative forcing associated with low and high clouds in the Tropics and changing the area of the convective region. The interaction of the convective and subsidence regions of the Tropics and related changes in temperature, moisture, and circulation are discussed. In particular, we find that boundary layer depth interacts strongly with free-troposphere hu-
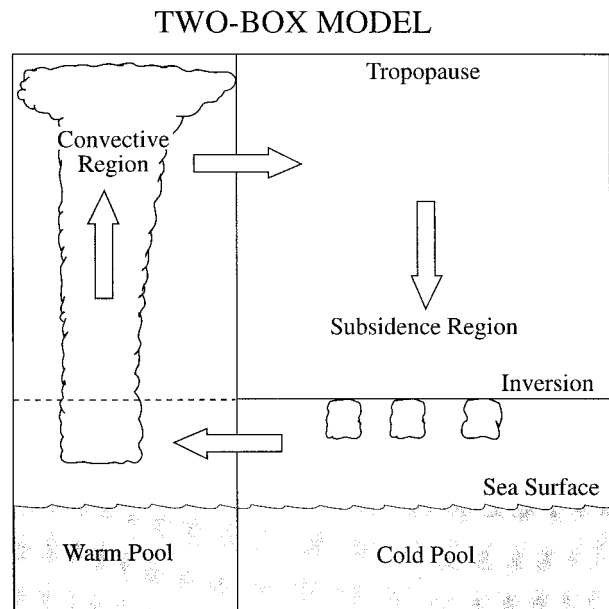
TWO-BOX MODEL

FIG. 1. Schematic of model. The warm pool has high convective clouds and the cold pool has boundary layer clouds. Air is rising in the warm pool and sinking across the inversion in the cold pool. The top of the energy balance model is at the tropopause.

midity in the subsiding region to produce a negative feedback.

2. Model description

a. Concept

A two-box energy balance model is shown schematically in Fig. 1. The convective region (warm pool box) refers to the region of the Tropics that has deep convection, high humidity throughout the depth of the atmosphere, and mean upward motion. In nature, the size and location of this region varies with season and on other timescales, but the relative area of the convective region is an externally specified parameter in this energy balance model. The subsidence region (cold pool box) is assumed to be that part of the Tropics with a trade inversion, descending dry air above the inversion, and some low clouds below the inversion, but no deep convection. We believe that this two-box structure captures a physically important aspect of the tropical climate in a very simple yet informative way.

The convective region atmosphere is assumed to be influenced by the deep convection, so the temperature profile there is fixed to a moist adiabat. Observations show the temperature profile in the Tropics closely approximates a moist adiabat (Xu and Emanuel 1989). The value of the moist adiabat is determined by the equivalent potential temperature of air near the sea surface of the convecting region. Using the small area of convecting clouds, Miller (1997) derived theoretically that in a two-box model the warm pool surface and tropo-

pause are linked by a moist adiabat. Other effects of convection are not explicitly treated.

Due to the very large tropical radius of deformation, the horizontal gradients in temperature across the Tropics above the boundary layer are small (Schneider 1977; Held and Hou 1980). Consequently we assume that the free-tropospheric temperatures in the warm and cold pool boxes are the same at every level above the inversion (Pierrehumbert 1995). The humidities in the two boxes are predicted from large-scale balance conditions.

The circulation in the model, composed of mean rising motion in the convective region and sinking motion in the subsidence region, approximates the Hadley and Walker circulations in the Tropics. For example, the warm pool may represent the region with the warmest water in the western tropical Pacific and Indian Oceans. We can think of the cold pool as the subsidence regions on all sides of the warm pool. The energy flux between the convective and subsidence regions is equal to the difference in energy between the upper and lower branches of the model circulation times the strength of the circulation. This large-scale circulation brings water vapor that is evaporated from the cold pool ocean to the convective region, where it is condensed and rained out. The return flow at upper levels brings much drier air with a higher total energy back to the cold pool. Because the moist static energy of the air exported to the cold pool is necessarily greater than the moist static energy of the air imported from the cold pool, the large-scale circulation removes heat from the convective box. Since the inflow to the warm pool is assumed to occur below the inversion, the strength of the circulation is driven by the subsidence at the top of the trade inversion, which is determined by the balance between radiative cooling and subsidence warming in the atmosphere above the inversion.

The model determines the equilibrium climate by requiring energy balance in both the atmosphere and ocean. Energy balance equations are applied for the boundary layer, the subcloud layer, the troposphere, and the entire column. Energy exports to the extratropics are prescribed for both the atmosphere and ocean.

One aspect of this model that differs from previous models of this type is that we predict humidity from moisture budget equations for each part of the model: the warm pool troposphere, the cold pool free troposphere, and the cloud-topped boundary layer. Although the integrated water is predicted, the humidity profiles in some regions are assumed. In the convective region the relative humidity is assumed constant with height throughout the atmosphere. This profile is in rough agreement with the mean relative humidity profile found during the active phase of the intraseasonal oscillation during the Tropical Ocean Global Atmosphere (TOGA) Coupled Ocean–Atmosphere Experiment field project (Brown and Zhang 1997). The specific value of relative humidity in the warm pool is predicted by the moisture budget. In the subsidence region the humidity above the
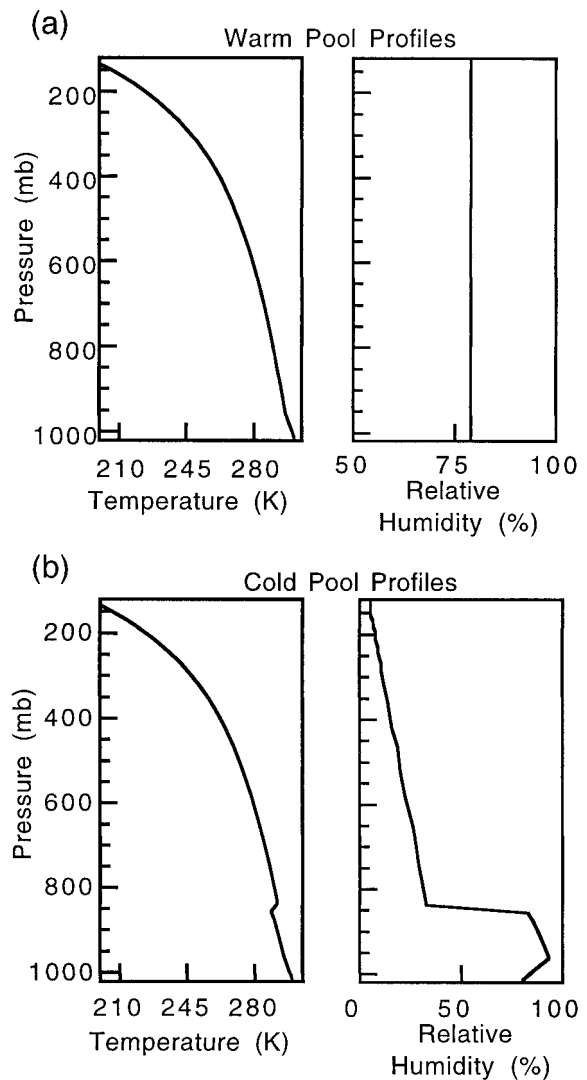

FIG. 2. Vertical profiles from control case with the relative area of the warm pool equal to 0.3333. (a) Temperature and relative humidity vertical profiles in the warm pool. (b) Temperature and relative humidity vertical profiles in the cold pool.

inversion is predicted from the moisture budget above the level of the inversion, but the profile is assumed, for simplicity, to be that specified by Manabe and Wetherald (1967). In principle, the humidity profile can be determined at every level above the inversion from our equations, but we have not implemented that feature. Figure 2 shows the temperature and relative humidity profiles for the base case in the convective and subsidence regions.

To simulate the impact of clouds on this tropical equilibrium climate we specify the radiative properties of the anvils in the deep convective box and the boundary layer clouds in the subsidence region. High clouds with an optical depth of 6.5 cover 60% of the convective region in the base equilibrium climate. The properties are chosen to give approximately zero net cloud forcing

at the top of the atmosphere (TOA), as observed (e.g., Harrison et al. 1990; Hartmann et al. 1992). In the cold pool boundary layer (CPBL) a surface mixed layer is topped by a cloud layer with a fixed 30% cloud fraction and a fixed optical cloud depth of 5.0, giving a net cloud forcing at the TOA of -21 W m^{-2}. The top of the clouds is just below the trade inversion. These cloud properties and cloud radiative effects are in general agreement with International Satellite Cloud Climatology Project (ISCCP) and Earth Radiation Budget Experiment observations (Ockert-Bell and Hartmann 1992).

The amount of cloud cover in the subsidence region can be predicted by a diagnostic relationship. Klein and Hartmann (1993) developed a relationship between the low cloud cover and the lower tropospheric stability (LTS) in stratus regions. LTS is defined as the potential temperature at 700 mb minus the potential temperature at the surface. The relationship, $c' = 5.70$ LTS$'$, is used in this model. Here, c is the cold pool boundary layer cloud cover in percent and the primes refer to anomalies from the average (base case) value. Miller (1997) also used this relationship to predict low cloud amount in a two-box model. Miller found that this relationship leads to a negative feedback associated with the low clouds.

The model uses two boxes in the Tropics as in Pierrehumbert (1995), though it includes more realistic radiation fluxes and a boundary layer in the cold pool. The boundary layer uses a mixing line model based on Betts and Ridgway (1988, 1989, hereafter BR89). Unlike the two-box model in Miller (1997), this model predicts the height of the boundary layer and the amount of water vapor above the cold pool inversion. The two-box model of Clement and Seager (1999, manuscript submitted to *J. Climate*), differs from this model because it has a fixed ratio of warm pool to cold pool area and interactive ocean heat transports.

By requiring energy and moisture balances in the atmosphere and the ocean, we are able to determine solutions for the dependent variables of the model: the sea surface temperatures in the cold and warm pools, the strength of the circulation, the temperatures and humidities in the atmosphere, and the height of the trade inversion. This equilibrium climate is a function of the independent variables in the model, which include the relative size of the warm and cold pools, the surface wind speed, the cloud fractions, and others. We will test the sensitivity of the model climate to these parameters. Specific model details are given in the following sections.

b. Cold pool boundary layer equations

This section describes the heat and moisture balances used below the trade inversion in the subsidence region. In the mixing line model, a mixed layer extends from the surface to the lifting condensation level of surface air, and above that a cloud layer extends to the trade inversion. The air properties in the cloud layer are determined by conservative mixing of air from above the inversion with surface air (BR89).

The moisture balance states that the drying of the CPBL due to the entrance of dry subsiding air into the CPBL is balanced by evaporation at the ocean surface. The energy balance of the CPBL, where no precipitation is assumed to occur, requires that the radiative cooling of the CPBL is balanced by the warming due to subsidence of air through the trade inversion plus the small surface sensible heat flux. For the CPBL, the moist and dry static energy balances are

$$Lm_c(\overline{q} - q_{invp}) = F_{evap}^c, \qquad (1)$$

$$c_p m_c(\theta_{invp} - \overline{\theta}) + F_s^c = \Delta R_{inv}. \qquad (2)$$

Here θ is the dry potential temperature and q represents the specific humidity. The variables representing properties of air above the inversion have the subscript invp (inversion plus). Also, c_p is the specific heat of air and L is the latent heat of vaporization of water. Finally, m_c refers to the strength of the subsidence at the top of the inversion, and by continuity it equals the mass flow from the cold pool to the warm pool below the inversion, assuming no net exchange of mass from the extratropics. The overbar symbol indicates the pressure weighted mean in the CPBL; for example,

$$\overline{q} = \frac{1}{(p_{sfc} - p_{inv})} \int_{p_{inv}}^{p_{sfc}} q \, dp. \qquad (3)$$

In (2), ΔR_{inv} refers to the net radiative flux divergence in W m^{-2} between the surface and the inversion with positive values indicating radiative cooling. Also, F_{evap}^c is the evaporation (latent heat flux) at the surface and F_s^c is the surface sensible heat flux. These quantities are defined using the bulk aerodynamic formulas:

$$F_{evap}^c = Lm_o(q_{sat} - q_{sfc}), \qquad (4)$$

$$F_s^c = c_p m_o(\theta_{SST} - \theta_{sfc}), \qquad (5)$$

$$m_o = \rho C_d V_{surf}. \qquad (6)$$

Here q_{sat} is the saturation vapor pressure at the sea surface and θ_{SST} is the potential temperature at the sea surface. Further, m_o refers to the mass flux at the surface; it is proportional to the surface wind speed, V_{surf}, and density, ρ, with $C_d = 0.0013$. At the surface the variables are specified by subscripts sfc.

To determine the vertical profile of specific humidity and temperature in the boundary layer, two mixing line model parameters are needed. The first, β (dp^*/dp), is the change in lifting condensation level (p^*) with pressure and it is set to 1.2 for the marine stratocumulus clouds. The second, α, is the change in virtual potential temperature with height and is set to -2.832 K (100 mb)$^{-1}$ (Betts 1985).

In the subcloud layer, the radiative cooling, sensible heat flux at the surface, advection into the layer, and the buoyancy flux must balance. Here the advection term

is neglected, since it is an order of magnitude smaller than the other terms. The buoyancy flux at the top of the well-mixed subcloud layer is scaled to be proportional to the surface sensible heat flux. Thus we have a relation coupling the surface heat flux directly to the radiative cooling in the subcloud layer:

$$(1 + K)c_p m_o (\theta_{\text{SST}} - \theta_{\text{sfc}}) = \Delta R_{\text{sc}}. \quad (7)$$

The constant K is set to 0.25. Here ΔR_{sc} refers to the net radiative flux divergence in W m^{-2} between the surface and the lifting condensation layer with positive values indicating radiative cooling. This equation closes the system and the surface air temperature, humidity, and inversion height can all be predicted in the CPBL.

These mixing line model equations equilibrate on the timescale of approximately 1 day. Some of the quantities that must be specified to solve the mixing line equations are the moist adiabat that the temperature profile adheres to above the inversion, the subsidence strength, the SST, and the profile of upper-tropospheric humidity. The sensitivity of the mixing line model to these parameters is important in interpreting the coupled model behavior. For example, increasing the SST increases the sensible and latent heat fluxes and increases the height of the trade inversion. Increasing the surface wind speed increases the height of the trade inversion, the specific humidity near the surface, and the latent heat flux. Using a warmer upper-tropospheric moist adiabat lowers the inversion height. Increasing the specific humidity above the inversion affects Eq. (1); as q_{invp} increases, $\overline{q}$ also increases by lowering cloud top, since specific humidity is higher near the surface. Also, the latent heat flux decreases and the humidity at the surface increases for this case. Increasing the subsidence rate lowers the inversion height and increases the sensible and latent heat fluxes.

c. Tropospheric energy balance equations

The energy balance for the troposphere is used to constrain the values of the moist adiabat and subsidence strength. For the sum of the subsidence region and convection region troposphere, the net radiative cooling of the atmosphere and export of heat to the extratropics balances the latent plus the sensible heat fluxes at the sea surface:

$$a_c F_{\text{evap}}^c + a_w F_{\text{evap}}^w + a_c F_s^c + a_w F_s^w$$
$$= a_c \Delta R_{\text{trop}}^c + a_w \Delta R_{\text{trop}}^w + F_{\text{aex}}. \quad (8)$$

The equation includes contributions from the fluxes in both the warm (with a superscript w) and cold (superscript c) pool boxes. Here ΔR_{trop} is the net radiative flux divergence in the atmosphere between the tropopause and the sea surface. Also, a_c is the fractional area of the cold pool box and a_w is the fractional area of the warm pool box ($a_c + a_w = 1$). Finally, F_{aex} is the atmospheric export to midlatitudes (-19.5 W m^{-2}). As

in BR89, the tropopause is approximated by the level where the moist adiabat intersects the 195 K isotherm.

The atmospheric energy flux (Flux) between the two boxes is proportional to the strength of the circulation times the difference in equivalent potential temperature between the CPBL mean and the warm pool mean above the height of the cold pool inversion:

$$\text{Flux} = c_p(a_w \overline{m_w \theta_e^w} - a_c \overline{m_c \theta_e^c}), \quad (9)$$

$$\overline{m_w \theta_e^w} = \int_{p_{\text{inv}}}^{p_{\text{trp}}} \frac{\partial m_w}{\partial p} \theta_e^w \, dp$$

$$\overline{m_c \theta_e^c} = \int_{p_{\text{sfc}}}^{p_{\text{inv}}} \frac{\partial m_c}{\partial p} \theta_e^c \, dp. \quad (10)$$

The energy and moisture fluxes between the boxes can depend on the divergence profile ($\partial m / \partial p$). In the CPBL, the divergence is assumed to be independent of pressure. In the base case, the divergence above the inversion also is assumed to be independent of pressure. Other divergence profiles for the warm pool are explored in the moisture budget section below.

The tropospheric energy balance equation in the subsidence region is

$$F_{\text{evap}}^c + F_s^c + \frac{\text{Flux}}{a_c} = \Delta R_{\text{trop}}^c + \frac{F_{\text{aex}}}{a_c}, \quad (11)$$

where F_{evap}^c is the surface latent heat flux and F_s^c the sensible heat flux in the subsidence region. Further, ΔR_{trop}^c is the net radiative flux divergence in the cold pool troposphere.

The warm pool heat balance is similar to (8):

$$F_{\text{evap}}^w + F_s^w - \frac{\text{Flux}}{a_w} = \Delta R_{\text{trop}}^w. \quad (12)$$

d. Ocean energy balance equations

The oceanic energy balance is straightforward:

$$a_c F_{\text{evap}}^c + a_w F_{\text{evap}}^w + a_c F_s^c + a_w F_s^w$$
$$= a_c R_{\text{sfc}}^c + a_w R_{\text{sfc}}^w - F_{\text{oh}}, \quad (13)$$

where R_{sfc} refers to the net downward radiation at the surface, and F_{oh} is the energy export from the tropical ocean into the midlatitude ocean. The energy balance for the entire system can be obtained by combining (11), (12), and (13),

$$a_c R_{\text{TOA}}^c + a_w R_{\text{TOA}}^w = F_{\text{aex}} + F_{\text{oh}}, \quad (14)$$

where R_{TOA} represents the net shortwave plus longwave radiation entering the top of the atmosphere. By incorporating the atmospheric flux term, the SSTs in the convective and subsidence regions are constrained separately:

$$R_{\text{TOA}}^c + \frac{\text{Flux}}{a_c} = \frac{F_{\text{aex}}}{a_c} + F_{\text{oh}}^c, \qquad (15)$$

$$R_{\text{TOA}}^w + \frac{\text{Flux}}{a_w} = F_{\text{oh}}^w. \qquad (16)$$

The oceanic export to midlatitudes is split up to the warm pool and cold pool components, with superscripts w and c respectively, and they are related by

$$a_c F_{\text{oh}}^c + a_w F_{\text{oh}}^w = F_{\text{oh}}. \qquad (17)$$

e. Moisture budget equations

This moisture budget differs from those found in previous two-box models (Pierrehumbert 1995; Miller 1997). Specifically, here the water vapor in the upper troposphere of the cold pool is predicted. The moisture budget is formulated for five regions: the sea surface, above the inversion in the cold pool, the CPBL, the warm pool above the level of the cold pool inversion, and the warm pool below that level. The moisture balance in the CPBL was already described in section 2c.

At the sea surface total evaporation is equal to the precipitation in the warm pool:

$$a_c E^c + a_w E^w = a_w P. \qquad (18)$$

The precipitation rate in the warm pool is 14 mm day^{-1} for the base case. This corresponds to an average precipitation rate of about 1.7 m yr^{-1} over the model domain.

In the warm pool below the level of the cold pool inversion, moisture is imported from the cold pool ($F_q^{\text{BL}} = L\overline{q}a_c m_c$) and through evaporation from the sea surface, and moisture is exported by ascent across the inversion (F_{inv}^w), so that in equilibrium,

$$F_q^{\text{BL}} + a_w E^w - F_{\text{inv}}^w = 0. \qquad (19)$$

The moisture imported from the CPBL is the same amount exported from the CPBL, as seen in Eq. (1).

Above the level of the cold pool inversion in the warm pool, the precipitation plus the amount of moisture exported to the cold pool (F_q^{trp}) equals the moisture flux ascending in the warm pool at the level of the cold pool inversion (F_{inv}^w),

$$F_{\text{inv}}^w - F_q^{\text{trp}} - a_w P = 0. \qquad (20)$$

The upward flux of moisture in the warm pool is assumed to be proportional to the large-scale mass flux:

$$F_{\text{inv}}^w = a_w m_w L q_{\text{inv}}^w (1 + \gamma), \qquad (21)$$

where q_{inv}^w is the specific humidity in the warm pool at the level of the cold pool trade inversion. The parameter γ represents the fraction by which eddy fluxes augment the large-scale flux. A reasonable climate is obtained if the value of γ is set to 0.44. The relative humidity in the warm pool is determined from (21). The constant γ is a key closure parameter for the moisture budget and is a great simplification over more detailed physical

models that parameterize detrainment, between-cloud subsidence, and precipitation efficiency within the warm pool.

In the atmosphere above the inversion in the cold pool, all the moisture is assumed to come from the warm pool and descend across the inversion. Salathe and Hartmann (1997) have shown with observations that the upper-tropospheric water vapor is well predicted by the large-scale advection of water vapor from convective regions. Liquid water and ice advection do not appear to be important. We neglect moisture exchange with the extratropics. So the vapor leaving the warm pool (F_q^{trp}) must equal the vapor crossing the inversion in the cold pool (F_{inv}^c):

$$F_{\text{inv}}^c = F_q^{\text{trp}} \qquad (22)$$

$$a_c m_c L q_{\text{invp}} = a_w L \int_{p_{\text{inv}}}^{p_{\text{trp}}} \frac{\partial m_w(p)}{\partial p} q_w(p)\, dp, \qquad (23)$$

where q_{invp} is the specific humidity immediately above the cold pool inversion. Also, m_c is the subsidence in the cold pool at the level of the trade inversion, m_w is the rising motion in the warm pool, and q_w is the amount of water vapor in the warm pool for each pressure level. The mass of air subsiding at the inversion of the cold pool is equal to the air rising in the warm pool at the same level:

$$a_w m_w = a_c m_c. \qquad (24)$$

Assuming constant divergence of warm pool air between the trade inversion and the tropopause, (23) becomes

$$q_{\text{invp}} = \overline{q_w} = \frac{1}{p_{\text{inv}} - p_{\text{trp}}} \int_{p_{\text{inv}}}^{p_{\text{trp}}} q_w(p)\, dp. \qquad (25)$$

For constant divergence, the amount of moisture immediately above the trade inversion is equal to the pressure-weighted mean moisture in the warm pool above the inversion. Note that the moisture in the cold pool does not depend directly on the strength of the circulation or the ratio of the areas of the cold pool to warm pool. It is the humidity of the warm pool that is important. Equation (23) can be solved for any pressure below the tropopause and above the inversion in the cold pool, giving the humidity profile above the trade inversion in the cold pool. For simplicity, we have solved it only at the inversion and assumed the Manabe and Wetherald (1967) profile above that level. This moisture budget is in contrast to Sun and Lindzen (1993), who proposed that hydrometeors from the convective region are the strongest contributors to the upper-tropospheric humidity in subsidence regions.

We get reasonable humidities in the cold pool troposphere by assuming a large-scale divergence profile that is independent of pressure. With our assumption of constant divergence from inversion to tropopause, a humidity of 5.3 g kg^{-1} above an inversion at 850 mb is obtained in the cold pool, which compares well with

TABLE 1. Boundary layer results for changing divergence profiles.

Divergence profile	Warm pool SST (K)	Cold pool SST (K)	Pressure at the inversion (mb)	Specific humidity above inversion (g kg^{-1})	Strength of subsidence at inversion (mb day^{-1})
Constant	302.9	300	850	5.3	52.4
Linearly decreasing from tropopause to 700 mb	298	292.4	875	0.83	55.8
Linearly decreasing from tropopause to 400 mb	299.3	295.0	750	0.20	52.2
Linearly decreasing from tropopause to 300 mb	300.1	296.1	690	0.07	49.7

data in Betts and Albrecht (1987). The observed divergence profile, on the other hand, is strongly peaked in the upper troposphere (Mapes and Houze 1995). If we approximate this divergence profile by one that is maximum at the tropopause and decreases linearly to zero at 400 mb, we obtain a specific humidity of 0.2 g kg^{-1} above an inversion at 750 mb (Table 1). In this case the cold pool is unrealistically dry and the inversion is high. (Other profiles of divergence are included in Table 1.)

In reality, the exchange of moisture between the warm pool and the cold pool is not determined by the mean divergent circulation alone. Mixing by transient and nondivergent motion is also important (Yang and Pierrehumbert 1994). The successful simulation given by the constant divergence profile assumes that water vapor is mixed into the subsiding regions from all levels of the convective region. A constant divergence is equivalent to letting all levels contribute water vapor in proportion to their mass, and this is in many ways the simplest assumption. Our constant divergence profile is a simple way of producing realistic values of cold pool humidity.

f. Solution procedure

Model solutions are obtained by an iteration procedure. Initially a solution to the model is guessed, then the terms of the equations are computed and checked. The equations are checked in a specific order and the first variables are changed until the first equation balances, before the next equation is evaluated. Every time a variable is changed, the model solution is checked again from the beginning. The surface specific humidity and surface air temperature in the cold pool and the trade inversion height are adjusted until Eqs. (1), (2), and (7) are satisfied. Equations (21) and (23) constrain the humidities in both pools. The ocean energy balance

TABLE 2. External parameter values for base case.

Parameter	Value in base case
Cold pool surface wind speed	6.7 m s^{-1}
Warm pool surface wind speed	4.2 m s^{-1}
Atmospheric export to extratropics	−19.5 W m^{-2}
Ocean export to extratropics	−42.5 W m^{-2}
Relative area of warm pool	0.3333
Relative area of cold pool	0.6667
High cloud cover in warm pool	60%
BL cloud cover in cold pool	30%

in the warm pool and Eqs. (8), (11), and (14) are iterated toward equilibrium by adjusting the SST in the warm and cold pools, the strength of the subsidence, and the value of the moist adiabat. Convergence is assumed when the energy and moisture balances are all within 1% of the largest energy term in the equation. The uncertainty in the SST with this constraint is 0.5 K. The radiation code STREAMER (Key 1996 and references therein) is used to determine the radiative fluxes. The two-steam radiative approximation is used and the radiative effects of principle gases, carbon dioxide, ozone, water vapor, and the specified clouds are included.

3. Model sensitivities

In this section the base model and its sensitivities to some of the parameters will be described and explored. The area ratio, surface wind speed, and cloud cover are changed in small increments and the subsequent changes in the model equilibrium are described. In addition, we investigate the role of humidity above the boundary layer in the cold pool and the role of the moisture prediction equations as the area ratio is changed. The response of two-box models to clouds and area ratios has been previously studied (Miller 1997; Pierrehumbert 1995). Here the response of the circulation strength, as given by the subsidence strength at the height of the variable trade inversion, is also noted.

a. Base climate

For the base case, the parameters are chosen to approximate the Walker circulation in the Pacific (Table 2). This system is now relatively well observed, especially from the TOGA Tropical Ocean Atmosphere (TAO) buoy array. The base case parameters are evaluated by supposing the model covers the area in the Pacific observed by the TAO buoys, 10°N–10°S and 135°E–95°W. The warmest waters, and high humidities and upper-level cloudiness, cover the western third of the region, so the relative area of the warm pool in the base case is 0.33 and cold pool relative area is 0.67.

Values for the ocean and atmospheric exports across 10°N and 10°S are 42.5 and 19.5 W m^{-2}, respectively (Peixoto and Oort 1992). The surface wind speed in the warm pool is set to 4.2 m s^{-1} and in the cold pool to 6.7 m s^{-1}. The surface wind speeds are consistent with

TABLE 3. Base case solution state variables.

Variable	Value in base case
SST warm pool	302.9 K
SAT warm pool	300.8 K
SST cold pool	300.0 K
SAT cold pool	299.0 K
Inversion pressure	850 mb
Specific humidity above inversion	5.3 g kg^{-1}
Relative humidity in warm pool	78%
Subsidence at inversion	52 mb day^{-1}
Value of moist adiabat	354 K
Mean precipitation rate in tropics	4.6 mm day^{-1}
Latent heat flux in warm pool	124 W m^{-2}
Latent heat flux in cold pool	133 W m^{-2}

FIG. 3. SST vs relative warm pool area. Warm pool SST is dashed and the cold pool SST is solid.

data from the Comprehensive Ocean–Atmosphere Data Set, where the wind speeds in the warm pool are less than in the cold pool. Higher cold pool surface winds speeds are also found by the TOGA TAO buoys from July 1991 to June 1993 (Zhang and McPhaden 1995). Convective cloud cover is chosen to be 60% in the warm pool and boundary layer cloud cover is 30% in the cold pool, in agreement with ISCCP estimates.

The ocean heat transport divergence is taken from Hartmann (1994, Fig. 4.18). The cold pool region is influenced by larger oceanic cooling from the upwelling that occurs in the eastern Pacific ocean. The oceanic export was distributed between the warm and cold pools as consistent with Hartmann (1994); 5 W m^{-2} is exported from the warm pool ocean and 61.25 W m^{-2} is exported from the cold pool ocean. The tropical western Pacific is surrounded by subsidence regions so atmospheric export to the extratropics is applied only to the cold pool region. The subsidence region exports 19.5/0.67 = −29.25 W m^{-2} to the extratropics in the base case.

The model equilibrium values for the base case are given in Table 3. The observed annually averaged SST in the western Pacific is 303.1 K and in the east is 299.2 K (Reynolds and Smith 1995). The model temperatures are 302.9 and 300 K, respectively. The inversion is usually found around 800 mb in the trade wind regime of the Pacific and it is at 850 mb in this model. The relative humidity in the warm pool is expected to be around 75% from the warm pool observations in Brown and Zhang (1997) and here it is 78%. A reasonable observed value of the specific humidity above the inversion is 4 or 5 g kg^{-1}, and it is 5.3 g kg^{-1} in this model. The subsidence rate at the inversion should be about 40 mb day^{-1} (Betts and Ridgway 1988) and it is 52 mb day^{-1} here. The TOGA TAO buoys show latent heat flux in the warm pool of 93 W m^{-2} and cold pool latent heat flux of 98 W m^{-2} when averaged from July 1991 to June 1993 (Zhang and McPhaden 1995). This model gives slightly higher latent heat fluxes of 124 W m^{-2} in the warm pool and 133 W m^{-2} in the cold pool. The mean tropical precipitation in the model is 4.6 mm day^{-1}, which is approximately the tropical average an-
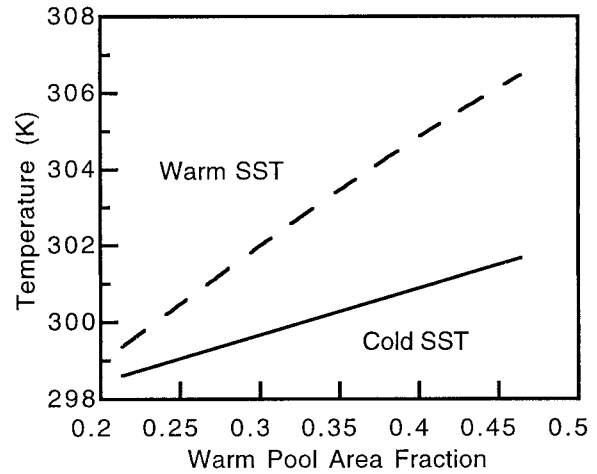
nual mean precipitation between 10°N and 10°S (Peixoto and Oort 1992). Also, BR89 give a value of 348.6 K for the tropical moist adiabat, which is close to the 354 K in the base case equilibrium.

b. Area ratio and moisture budget

How would the tropical SSTs evolve if the area of the deep-convective portion of the tropics increased? To investigate this we performed a series of calculations in which the area of the warm pool was varied (Fig. 3). The cloud cover in each box was adjusted to keep the total tropical amount of high and low clouds constant as the relative areas changed. Tropical cloud forcing at the TOA stays constant when the tropical cloud amount is constant. As the convecting region increases in area, the SSTs in both regions increase. The temperatures increase because the low humidity of the upper troposphere in the subsidence region is replaced with the high humidity of the convecting region. As the humid convective region occupies a larger fraction of the Tropics, warmer temperatures are needed to emit the same amount of energy to space. This same effect is described in Pierrehumbert (1995).

The area ratio was varied with two different moisture schemes. For the fixed humidity experiment the relative humidity in the warm pool and the specific humidity above the inversion of the cold pool were both held constant at their values for the base case. Equations (21) and (25) were not used for the fixed humidity experiment. In the moisture budget experiment the warm pool relative humidity increases from 72% to 86% and the specific humidity above the cold pool inversion changes by 4 g kg^{-1}, which corresponds to an increase in the relative humidity above the inversion from 30% to 39% (Fig. 4).

The cold pool subsidence rate decreases with its relative area using both fixed and predicted moisture (Fig.
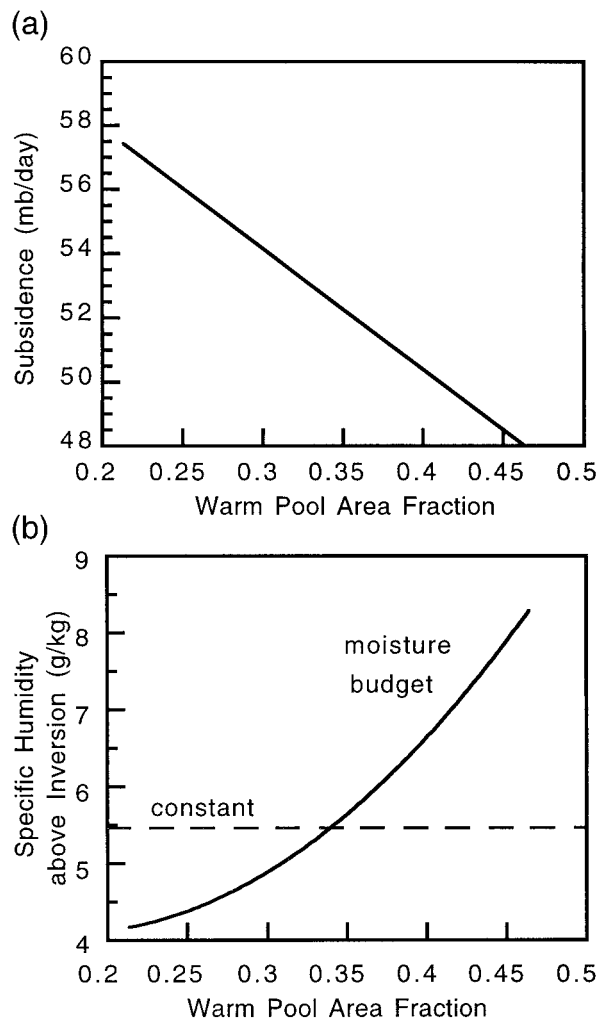
(a)

(b)

FIG. 4. Variable sensitivities as the relative area of the warm pool increases. (a) Subsidence, strength of the circulation. (b) Specific humidity above the trade inversion in the cold pool. Solid line is for predicted moisture and dashed line is for fixed humidity.
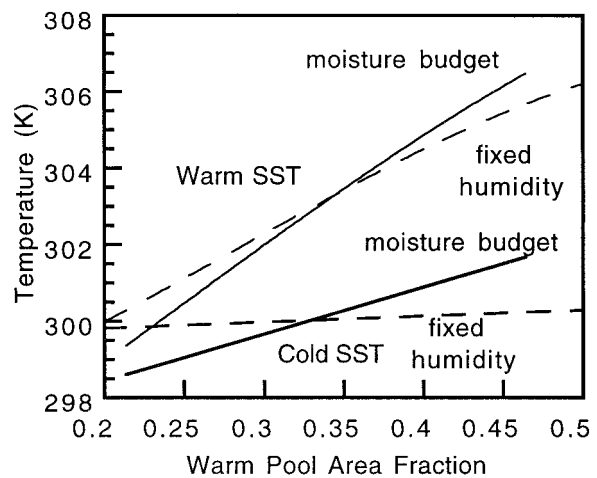

FIG. 5. Comparison of equilibrium solutions for experiments using the moisture budget (solid) and for experiments when the humidity is specified as a constant (dashed). The warm pool SST (thin) and cold pool SST (thick) are shown.

4). The subsidence in the cold pool is equal to the radiative cooling of the atmosphere divided by the dry static stability for that region. The dry static stability is related to the lapse rate of the moist adiabat. Because the moist adiabatic lapse rate strongly decreases with increasing temperature, the dry static stability of the troposphere rises dramatically in a warmer climate. The dry static stability increase dominates the change in radiative cooling, leading to a decrease in the strength of the subsidence. Knutson and Manabe (1995) also found a decrease in the tropical circulation and an increase in static stability when the climate in their coupled GCM was warmed by doubling CO_2. Both the subsidence and the cold pool area decrease as the relative area of the warm pool increases, so the large-scale mass flux decreases with increasing warm pool area. In a fully coupled model in which the convective area is predicted, these effects may lead to a negative feedback that con-

strains the size of the convective area. In this experiment the SST difference increases as the circulation and associated large-scale heat flux decrease. This is logical from a thermodynamic perspective, but we might get a different result in a model with a momentum budget. The increasing difference between the cold pool and warm pool SSTs is also found in Pierrehumbert (1995).

The large-scale energy flux between the boxes is proportional to the strength of the circulation times the difference in mean equivalent potential temperature between the CPBL and the warm pool troposphere. The strength of the circulation decreases as the warm pool area is made bigger, and the difference in mean equivalent potential temperature increases somewhat to maintain the energy exchange rate (Fig. 4). The mean equivalent temperature in the CPBL increases more than the SST indicates because the height of the inversion decreases 60 mb, and equivalent potential temperature decreases with height in the mixing line boundary layer in the moisture budget case. The warm pool tropospheric equivalent potential temperature rises because the relative humidity in the warm pool increases 15%. These factors increase the energy transport per unit of large-scale mass flux, and the amount of large-scale mass flux decreases strongly with the increase in warm pool relative area. In the constant moisture case, the inversion height remains constant and the SST difference between the two pools is more sensitive to changes in area ratio than in the moisture budget case. Since the CPBL height is less sensitive with fixed humidity and the warm pool relative humidity is fixed, the SST difference increases to create the same mean equivalent potential temperature difference as in the moisture budget case.

Using a moisture budget causes a positive feedback, when compared with a fixed humidity experiment (Fig. 5). In the moisture budget experiment the increase in
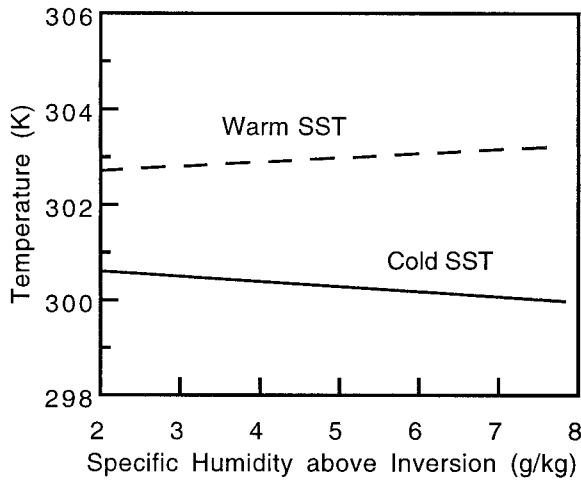
FIG. 6. SST in the warm and cold pools vs specific humidity above the inversion. Warm pool SST is dashed and the cold pool SST is solid.

FIG. 7. Height of the inversion vs the specific humidity above the inversion.

temperature of the moist adiabat leads to an increase in the cold pool specific humidity above the inversion. The moist adiabat requires that a small warming at the surface is magnified in the upper troposphere. The warmer temperatures in the warm pool upper troposphere require more specific humidity to maintain similar warm pool relative humidities. The humidity above the inversion in the cold pool is a slave to the warm pool specific humidity, so the cold pool humidity increases with temperature.

c. Moisture budget: Cold pool humidity

The sensitivity of the model to the specific humidity above the inversion is very interesting. The moisture budget is suppressed in the following experiment by keeping the relative humidity in the warm pool constant. Equations (21) and (25) are disabled and the specific humidity above the inversion is fixed at values varying from 2 to 8 g kg^{-1}. Surprisingly, the SSTs in the model stay nearly constant as the moisture is varied (Fig. 6). In a sequence of equilibrium calculations, the outgoing longwave radiation (OLR) above the cold pool is surprisingly insensitive to the humidity above the inversion. The reason for this is the response of the mixing line model to the increased humidity. As the humidity above the inversion increases, the CPBL thins significantly (Fig. 7). The expected decrease in OLR due to enhanced upper-tropospheric water vapor is almost cancelled by two factors. The factors are the decrease in the amount of boundary layer water vapor and the increase of the average temperature of the water vapor content of the boundary layer. The greenhouse effect of water vapor in the Tropics is largely contributed by lower-tropospheric water vapor (Shine and Sinha 1991). If this compensation between humidity above the inversion and thickness of the boundary layer actually
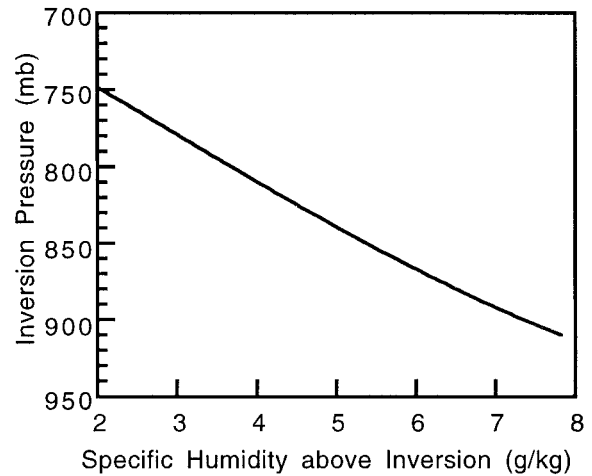
operates in nature, it could constitute an important negative feedback for the climate system, and it might make upper-tropospheric humidity in subsidence regions of the Tropics a less critical issue.

The compensation arises from the energy and moisture budget equations for the boundary layer. If the humidity above the inversion is increased, it causes the radiative cooling of the boundary layer to decrease. From (2), a new equilibrium can be achieved for fixed mass flux by decreasing the difference between potential temperature above the inversion and the mean potential temperature in the mixed layer. The difference is decreased by lowering the trade inversion. From (1), if we increase the humidity above the inversion, the moisture balance can be restored by increasing the mean humidity of the boundary layer. This is also achieved by moving the CPBL top down.

There are limitations of this model that may change this interesting behavior. In addition to the approximate nature of the mixing line model, we have assumed constant boundary layer cloud properties in these tests. The boundary layer cloud properties may change in a way that alters the negative feedback mechanism described here. Also, precipitation in the boundary layer could affect the equations in such a way as to reduce changes in inversion height. To see how precipitation in the CPBL could alter the sensitivity of inversion height to humidity above the inversion, rewrite (1) and (2) with a precipitation term included:

$$Lm_c(\overline{q} - q_{\text{invp}}) = F_{\text{evap}}^c - LP, \qquad (26)$$

$$c_p m_c(\theta_{\text{invp}} - \overline{\theta}) + F_s^c = \Delta R_{\text{inv}} - LP. \qquad (27)$$

Now begin as before with the fact that increased humidity above the inversion will decrease the radiative cooling of the boundary layer, and consider the implication of this for the energy budget in (27). Now the system can respond by either thinning the boundary
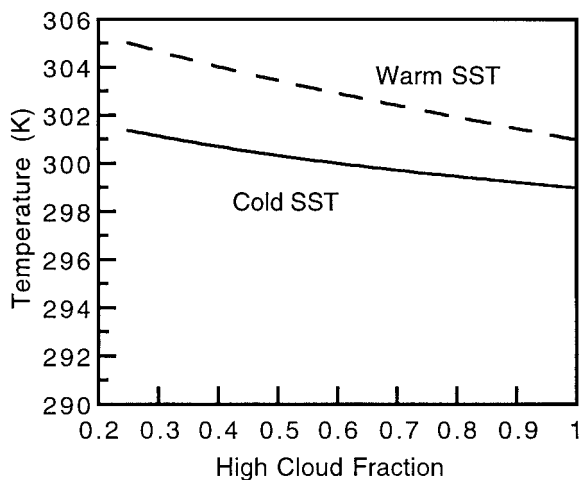
FIG. 8. SST vs warm pool cloud fraction. Warm pool SST is dashed and the cold pool SST is solid.

layer to decrease the entrainment heating, or by decreasing the precipitation rate, or both. Similarly, in the humidity equation (26), when the entrainment drying decreases with increased humidity above the inversion, the system can also achieve balance by decreasing the precipitation rate, lowering the inversion, or both. If precipitation in the boundary layer below the subsidence region is an important term in the heat and moisture budgets, then the sensitivity of the inversion height to moisture above the inversion might be less than in our model. The extent of the compensation provided by precipitation variations would need to be investigated with a model that captures the physics of precipitation in the boundary layer. The inclusion of precipitation has been explored by R. Seager and A. Clement (1998, personal communication).

d. Warm pool cloud sensitivity

The cloud cover in the convective region of the model is approximated by a high ice cloud of optical depth 6.5 covering 60% of the box with the cloud top at the tropopause. The amount of deep convection could change in a future climate regime, and it has been hypothesized that the radiative effect of clouds in convective regions could constitute a strong negative feedback on tropical SST (Ramanathan and Collins 1991). In this set of experiments the fractional area of clouds in the warm pool is changed from 25% to 100%, while keeping the other cloud properties fixed. Only the radiative effect of the clouds is considered. The warm pool SST shows a 1.7 K decrease in response to increasing the area coverage of convective clouds by 50% (Fig. 8).

The model shows little response to the radiative forcing of convective clouds because they do not significantly perturb the radiation balance at the TOA, where the shortwave and longwave effects (-94 and $+92$ W

m^{-2}, respectively, for the base case of 60% high cloud fraction) nearly cancel each other. This insensitivity is also found in the two-box models of Pierrehumbert (1995) and Miller (1997). The radiation balance at the surface of the warm pool is affected by the convective cloud amount because the convective clouds reduce insolation at the surface. The surface forcing affects the evaporation and sensible heat fluxes in the warm pool. As the convective cloud amount increases, the radiative heating of the surface decreases. From the warm pool part of (13) we see that decreased radiative heating of the surface can be balanced by decreased evaporation. In the troposphere (11) decreased total latent heat release is balanced by decreased longwave cooling of the atmosphere that is also produced by the convective clouds. When the cloud cover in the warm pool is increased from 25% to 90% the relative humidity in the warm pool decreases from 84% to 73%, the SST decreases by 3.7 K in the warm pool, and the difference between SST and surface air temperature (SAT) decreases from 4.2 to 0 K. The temperature changes offset the humidity changes and produce a 50 W m^{-2} decrease of latent heat flux. Thus the radiative effects of the high clouds within the system are almost completely cancelled by changes in the hydrologic balances, and these changes are accompanied by little change in SST. Because the radiative effects reduce evaporation and precipitation, the radiative changes seem to more strongly limit convection itself than SST. In this solution, the high cloud fraction increases as the total precipitation decreases. These trends are physically inconsistent and point to the need to determine the high cloud fraction with model variables. In a fully coupled model the radiative effects of clouds reduce the generation of convective instability and help establish a stable balance point in which convective clouds are limited in extent.

e. Cold pool boundary layer cloud sensitivity

The SST is much more sensitive to the amount of boundary layer cloud in the cold pool than to the amount of convective cloud in the warm pool, because the boundary layer clouds have a strong effect on the TOA energy balance. When the cold pool cloud fraction is varied from 20% to 90%, the cold pool SST decreases 12 K, the warm pool SST decreases 11 K, and the specific humidity at the top of the inversion decreases from 6.4 to 2.0 g kg^{-1} (Fig. 9). Contrasting figures 8 and 9 shows the insignificance of high warm pool clouds when compared to CPBL clouds. The increased CPBL cloud cover provides a strong cooling effect to the cold pool and this is quickly transmitted to the warm pool by the large-scale circulation. The cooling effect of low clouds was explored previously in a general circulation model (Philander et al. 1996) and a two-box model (Miller 1997).

The decreasing temperatures also imply a decreasing static stability in the cold pool free troposphere that is
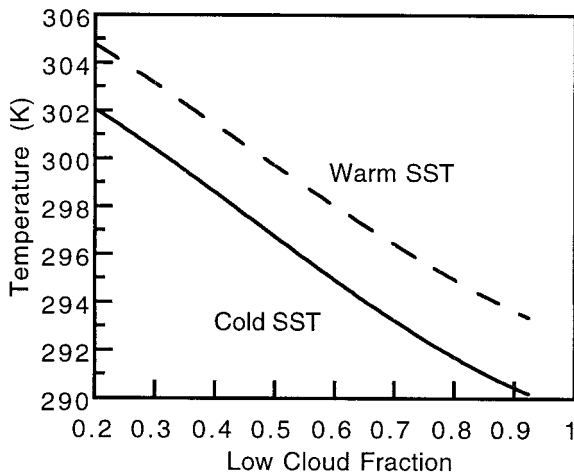
FIG. 9. SST vs varying cold pool cloud fraction. Warm pool SST is dashed and the cold pool SST is solid.

stronger than the decrease in radiative cooling above the cold pool inversion and produces an increase in the model circulation. The subsidence rate increases from 49 to 83 mb day^{-1} with increasing low cloud fraction because of the decreasing stability as the temperature of the moist adiabat decreases. The warm pool area and boundary layer (BL) cloud sensitivities both show that the static stability change is more important than the change in radiative cooling above the cold pool inversion.

f. CPBL predicted cloud fraction

When the CPBL cloud fraction is predicted from the LTS the model sensitivity is less than when the tropical average cloud fraction is kept constant (Fig. 10). Because we set the product of the area of the cloud cover and the relative area of each region to a constant means that the tropical average TOA cloud forcing is constant. LTS in the cold pool increases as the climate is warmed, because the temperature is assumed to follow a moist adiabat above the inversion. In the case where the climate is warmed by increasing the convective area, the SST difference between the two pools also increases slightly with temperature, and this also contributes to the LTS increase in the cold pool (Fig. 10a). Since the low cloud fraction is assumed to be proportional to LTS and the low clouds produce a cooling, the low cloud feedback will be strongly negative. When the cloud fraction is predicted from LTS, the temperatures are not as sensitive to the relative areas of the boxes (Fig. 10a). The cold pool SST increases for the constant tropical cloud fraction case, but decreases slightly for the predicted BL cloud fraction case. This negative feedback, also described in Miller (1997), could stabilize the tropical SSTs.
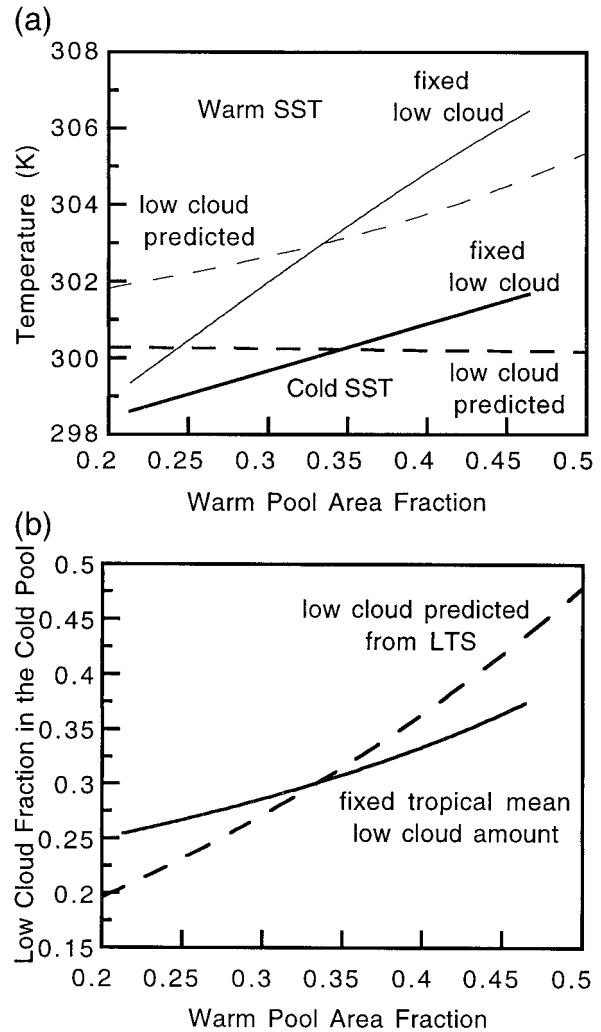

FIG. 10. (a) SST as a function of warm pool area for the warm pool (thin lines) and cold pool (heavy lines) for the cases in which tropical average low clouds in the cold pool are fixed (solid) and when the low clouds are predicted from lower-tropospheric stability (dashed). The tropical average low cloud amount is the area coverage of the low clouds in the cold pool times the relative area of the cold pool. (b) Warm pool area fraction vs CPBL cloud fraction while the BL cloud fraction is predicted using the LTS (dashed) and while the tropical average low cloud amount is held constant at 20% (solid).

g. Surface wind speed

In this model, the surface wind speed only affects the efficiency of the latent and sensible heat fluxes at the ocean surface. The surface wind speed is not coupled to the circulation in the model. In a set of experiments to test the sensitivity to wind speed, the surface wind speed is increased the same amount in both regions (the cold pool wind speed is shown in the figures and the warm pool wind speed is always 2.5 m s^{-1} less). The SSTs decrease as surface wind is increased, with the warm pool SST decreasing by a larger amount (Fig. 11). In the warm pool, the increased surface flux efficiency decreases the SST and decreases the relative humidity.
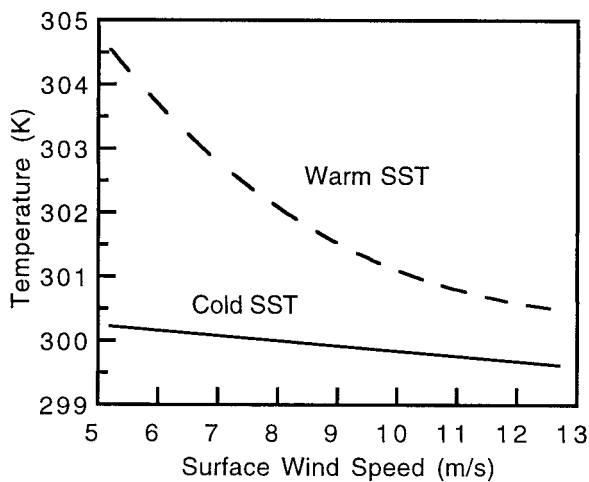
FIG. 11. SST vs surface wind speed. Warm pool SST is dashed and the cold pool SST is solid.

FIG. 12. (a) Profiles of equivalent potential temperature for different surface wind speeds: 5.2 m s^{-1} in cold pool (dashed) and 8 m s^{-1} surface wind speed in cold pool (solid). (b) Height of the cloud layer vs surface wind speed.

BR89 also found that increasing the wind speed decreased the SST, though the depth of the BL was constant in BR89 and in this experiment the CPBL depth increases with wind speed (Fig. 12b). The more efficient surface heat fluxes pump heat into the atmosphere. In the cold pool this energy flux can be balanced by decreasing the input of energy from the warm pool. The depth of the CPBL increases and the subsidence rate decreases, but the cold pool SST stays nearly constant as the wind speed is increased (Fig. 12a). A weaker circulation and smaller difference between cold and warm pool SSTs both decrease the energy flux to the cold pool from the warm pool. It is interesting to note that the large-scale energy flux makes it possible to increase the surface wind speed without decreasing the cold pool SST. This effect is not found in the one-box model of BR89.

As the wind speed is increased, the subsidence and the difference between the warm pool and cold pool SSTs both decrease. In this model the surface wind is not coupled to the circulation strength or the SST gradient. The sensitivities of the circulation and SST gradient to the surface wind speed suggest that a stable balance point would exist if the surface wind speed were coupled to the circulation strength and SST gradient. In such a coupled model, increased SST gradients would lead to increased circulation, which might lead to increased surface wind speed. According to the current model, the increased wind speed would act to decrease both the SST gradient and the circulation strength, leading to equilibrium. This behavior is similar to the mechanism described in Hartmann and Michelson (1993).

In one experiment the surface wind speed was made proportional to the strength of the circulation divided by the depth of the boundary layer. As the high cloud amount was changed, the SSTs and humidities in the model responded as if the wind speed was fixed.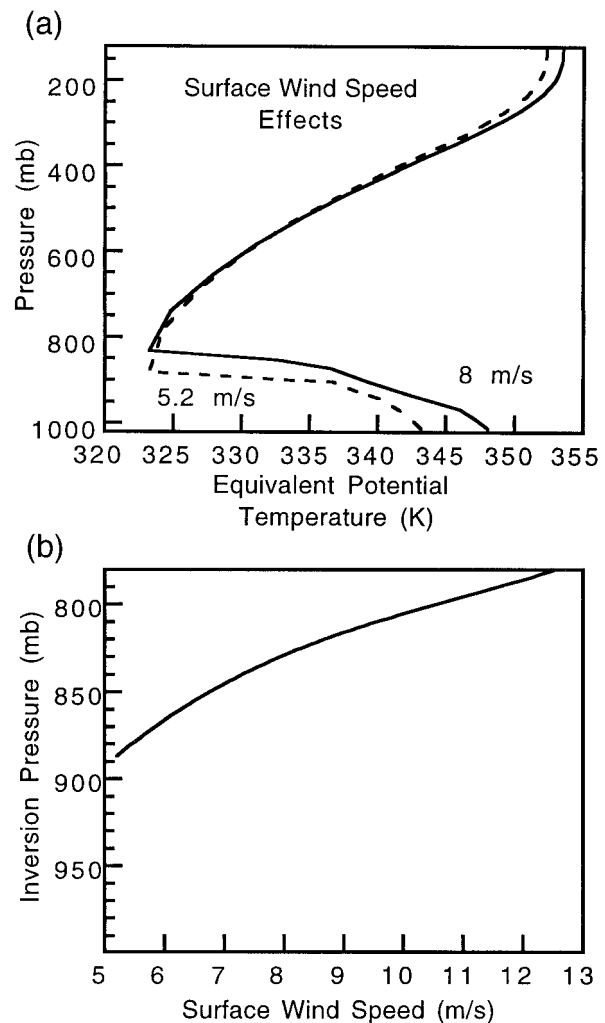 The circulation strength and inversion height did not vary as much with the predicted wind speed, and the predicted wind speed varied 0.5 m s^{-1} for the entire range of high cloud amounts. Predicting the surface wind speed, based on the divergent circulation, does not lead to significant changes in the sensitivity of the model to the high cloud amount, because the fractional change in the circulation strength is small.

4. Climate sensitivities to doubled carbon dioxide

To further investigate the sensitivity of the model, its response to doubled carbon dioxide (CO_2) is investigated. We investigate the effects of the moisture budget and the prediction of the CPBL cloud fraction by comparing with experiments in which the humidity and the low cloud fraction are fixed. To investigate these sensitivities, three pairs of doubled CO_2 experiments were conducted, as shown in Table 4. The first is a base case

TABLE 4. Change in tropical mean SST with doubled carbon dioxide.

Base case tropical mean SST	301 K
Doubled CO_2 and fixed humidity	+2.6 K
Doubled CO_2 with predicted humidity	+2.5 K
Doubled CO_2 with predicted humidity and low cloud feedback	+1.7 K

TABLE 5. Doubled carbon dioxide and moisture prediction.

Variable	Base case	Doubled CO_2 moisture budget	Doubled CO_2 fixed humidity
Tropical mean SST (K)	301	303.5	303.6
Inversion height (mb)	854	846	808
Specific humidity above inversion (g kg^{-1})	5.4	6.6	5.4
Subsidence rate (mb day^{-1})	52.4	48.8	45.3
Warm pool relative humidity (%)	79	79	79

in which the relative humidity in the warm pool and the specific humidity in the cold pool and the low cloud fraction are fixed at base values. In this case the model warms by 2.6 K. If the moisture prediction scheme is turned on, the warming is 2.5 K. Including the moisture budget does not have a significant effect on SST. Including the moisture budget does not change the relative humidity in the warm pool, but the specific humidity above the inversion in the cold pool is increased 1 g kg^{-1} (Table 5). From the moisture budget sensitivity experiment, an increase in specific humidity should thin the CPBL. The inversion is 37 mb lower in height in the doubled CO_2 moisture budget case than in the doubled CO_2 fixed humidity case. The inversion height is the same between the moisture budget cases with and without doubled CO_2, however, even though the specific humidity above the inversion is 1 g kg^{-1} higher in the doubled CO_2 case. The reason the mixed layer depth does not respond to the humidity as expected is because the subsidence rate also changes. The subsidence rate has a strong influence on the height of the BL with less subsidence, implying a thicker BL. The strength of the subsidence above the cold pool inversion decreases 7 mb day^{-1} when CO_2 doubles and moisture is predicted. This decrease occurs because the warmer moist adiabat increases the static stability in the upper troposphere of the cold pool more than the radiative cooling increases.

If the low cloud prediction scheme is turned on, the warming in response to doubled CO_2 is only 1.7 K. The low cloud fraction increases 3% in the cold pool as the carbon dioxide doubles, and this is enough to reduce the warming 0.8 K when compared to the case without low cloud feedback. This result is similar to that found by Miller (1997). As a 3% uncertainty in the percentage of low clouds is possible in current measurements, and 3% is enough to cause a half-degree negative feedback, the possibility of the low clouds affecting the climate of the Tropics is significant. It is uncertain to what extent the empirical correlation applies to the entire Tropics, since it was developed for stratus regions and a good fraction of the Tropics is in the trade cumulus regime rather than the stratus regime. It is interesting, however, that the relative humidity below the inversion in the CPBL increases with static stability, which is consistent with more cloud (Albrecht 1981; Bretherton et al. 1995).

5. Summary and conclusions

A simple two-box energy and moisture equilibrium model of the Tropics is used to investigate the physical mechanisms that control the climate of the Tropics. One box represents the convective region of the Tropics and the other box represents the subsiding regions in the Tropics. A large-scale circulation connects the heat and moisture budgets in the two boxes. The ratio of the areas of these two boxes must be specified, but the temperature and moisture are predicted. The temperature profile is assumed to follow a moist adiabat in the free atmosphere and the shape of the moisture profile is also prescribed, but the depth and properties of the boundary layer in the subsiding region are predicted with a mixing line model. Full radiative effects are included, but cloud optical properties are prescribed. A reasonable moisture prediction in the subsiding region is obtained if the convective region is assumed to detrain mass to the subsiding region in proportion to the vapor pressure at all levels.

If the fractional area of the convective region is increased, the climate warms, mostly as a result of the higher-tropospheric humidity in the convective region.

The humidity in the subsiding region above the inversion increases rapidly with temperature because it is slave to the humidity in the convective region, but the positive feedback from this is weaker than expected because the depth of the CPBL decreases significantly as the humidity above the inversion is increased. Much of the water vapor greenhouse effect comes from the boundary layer humidity, so it is quite sensitive to the inversion height.

The mass flux between the two regions decreases with increasing temperature because changes in the radiative cooling rate in the subsiding region are overwhelmed by changes in dry static stability associated with the assumed moist adiabatic lapse rate. The SSTs in the convective and subsiding regions are held close together by the strong sensitivity of the large-scale energy flux to the difference between the moist static energy of the air in the convective region and the moist static energy in the boundary layer of the subsiding region.

The radiative effects of convective clouds and boundary layer clouds produce very different responses in the model. Convective clouds have a small net radiative effect at the top of the atmosphere but cause a large redistribution of energy between the surface and the atmosphere. Because convection rapidly exchanges energy between the surface and the atmosphere in the

convective region, the importance of the convective cloud is dependent on its radiative forcing at the top of the atmosphere, which is small. So changing the area fraction of convective clouds has only a weak effect on equilibrium SST. The vertical redistribution of energy by convective clouds does have a significant influence on the hydrologic balances, since evaporation is reduced to compensate the reduction in solar heating of the ocean surface. This would have the effect of reducing the source of energy for convection. Thus, to first order, the radiative effects of convective clouds in the Tropics is to reduce the intensity of tropical convection, not to reduce the SST.

On the other hand, boundary layer clouds in the subsiding region are very important for SST because they have a strong influence on the net radiation at the top of the atmosphere. Increasing their fractional coverage strongly cools the climate. The change in static stability, driven by the decreasing moist adiabat, increases the strength of the circulation as the BL cloud cover increases, even though the net radiative cooling above the inversion in the subsiding region decreases.

If the cloud properties are fixed, the sensitivity of the model is close to that of a 1D model with fixed relative humidity. Doubled CO_2 increases the SSTs 2.6 K. If the boundary layer cloud in the subsiding region is predicted from an empirical relationship with lower-tropospheric static stability, a strong negative feedback is produced that cuts the sensitivity to doubled CO_2 by a third.

While this simple model is efficient and illustrates some important connections in the tropical climate, it is highly simplified and could be made more realistic in many ways. The model points to a key role for the boundary layer, and a critical question seems to be the ability of the mixing line model to predict changes in the depth of the CPBL in the subsiding region. Although thermodynamic models of the trade inversion height [Eq. (2)] do not include dynamic adjustments that horizontally flatten the trade inversion height (Schubert et al. 1995), they may still be of relevance for predicting climate variations in the mean trade inversion height. In view of the strong role of clouds in the boundary layer of the subsiding region, a boundary layer model that incorporates cloud prediction and explicitly includes precipitation and cloud radiative effects seems to be needed. A more sophisticated parameterization of the effect of convection on the temperature and humidity profiles in the convective region would also be helpful, perhaps coupled with a prediction of the cloud physical properties. Relaxing the assumption of no horizontal temperature variation above the mixed layer and including momentum constraints would also be desirable. Striking an appropriate balance between a model that is easily comprehended and one that is physically realistic is the key issue in mechanistic models of this type.

REFERENCES

Albrecht, B. A., 1981: Parameterization of trade-cumulus cloud amount. *J. Atmos. Sci.,* **38,** 97–105.

Betts, A. K., 1985: Mixing line analysis of clouds and cloudy boundary layers. *J. Atmos. Sci.,* **42,** 2751–2763.

——, and B. A. Albrecht, 1987: Conserved variable analysis of the convective boundary layer thermodynamic structure over the tropical oceans. *J. Atmos. Sci.,* **44,** 83–99.

——, and W. Ridgway, 1988: Coupling of the radiative, convective, and surface fluxes over the equatorial Pacific. *J. Atmos. Sci.,* **45,** 522–546.

——, and ——, 1989: Climatic equilibrium of the atmospheric convective boundary layer over a tropical ocean. *J. Atmos. Sci.,* **46,** 2621–2641.

Bretherton, C. S., E. Klinker, A. K. Betts, and J. A. Coakley, 1995: Comparison of ceilometer, satellite, and synoptic measurements of boundary-layer cloudiness and the ECMWF diagnostic cloud parameterization scheme during ASTEX. *J. Atmos. Sci.,* **52,** 2736–2751.

Brown, R. G., and C. Zhang, 1997: Variability of midtropospheric moisture and its effect on cloud-top height distribution during TOGA COARE. *J. Atmos. Sci.,* **54,** 2760–2774.

Clement, A. C., R. Seager, M. A. Cane, and S. E. Zebiak, 1996: An ocean dynamical thermostat. *J. Climate,* **9,** 2190–2196.

Fu, Rong, A. D. Del Genio, W. B. Rossow, and W. T. Liu, 1992: Cirrus-cloud thermostat for tropical sea surface temperatures tested using satellite data. *Nature,* **358,** 394–397.

Harrison, E. F., P. Minnis, B. R. Barkstrom, V. Ramanathan, R. D. Cess, and G. G. Gibson, 1990: Seasonal variation of cloud radiative forcing derived from the Earth Radiation Budget Experiment. *J. Geophys. Res. Atmos.,* **95** (D11), 18 687–18 703.

Hartmann, D. L., 1994: *Global Physical Climatology.* Academic Press, 411 pp.

——, and M. L. Michelsen, 1993: Large-scale effects on the regulation of tropical sea surface temperatures. *J. Climate,* **6,** 2049–2062.

——, M. E. Ockert-Bell, and M. L. Michelsen, 1992: The effect of cloud type on Earth's energy balance: Global Analysis. *J. Climate,* **5,** 1281–1304.

Held, I. M., and A. Y. Hou, 1980: Nonlinear axially symmetric circulations in a nearly inviscid atmosphere. *J. Atmos. Sci.,* **37,** 515–533.

Inamdar, A. K., and V. Ramanathan, 1994: Physics of greenhouse effect and convection in warm oceans. *J. Climate,* **7,** 715–731.

Key, J., 1996: Streamer user's guide. Tech. Rep. 96-01, Department of Geography, Boston University, 85 pp. [Available from Boston University, 121 Bay State Road, Boston, MA 02215.]

Klein, S. A., and D. L. Hartmann, 1993: The seasonal cycle of low stratiform clouds. *J. Climate,* **6,** 1587–1606.

Knutson, T. R., and S. Manabe, 1995: Time-mean response over the tropical Pacific to increased CO_2 in a coupled ocean–atmosphere model. *J. Climate,* **8,** 2181–2199.

Lau, K.-M., C. H. Sui, M. D. Chou, and W. K. Tao, 1994: An inquiry in to the cirrus-cloud thermostat effect for tropical sea surface temperature. *Geophys. Res. Lett.,* **21,** 1157–1160.

Manabe, S., and R. T. Wetherald, 1967: Thermal equilibrium of the atmosphere with convective adjustment. *J. Atmos. Sci.,* **24,** 241–259.

Mapes, B. E., and R. A. Houze Jr., 1995: Diabatic divergence profiles in western Pacific mesoscale convective systems. *J. Atmos. Sci.,* **52,** 1807–1828.

Miller, R. L., 1997: Tropical thermostats and low cloud cover. *J. Climate,* **10,** 409–440.

Ockert-Bell, M. E., and D. L. Hartmann, 1992: The effect of cloud type on Earth's energy balance: Results for selected regions. *J. Climate,* **5,** 1157–1171.

Peixoto, J. P., and A. H. Oort, 1992: *Physics of Climate.* American Institute of Physics, 520 pp.

Philander, S. G. H., D. Gu, D. Halpern, G. Lambert, N.-C. Lau, T. Li, and R. C. Pacanowski, 1996: Why the ITCZ is mostly north of the equator. *J. Climate,* **9,** 2958–2972.

Pierrehumbert, R. T., 1995: Thermostats, radiator fins, and the local runaway greenhouse. *J. Atmos. Sci.,* **52,** 1784–1806.

Ramanthan, V., and W. Collins, 1991: Thermodynamic regulation of ocean warming by cirrus clouds deduced from the 1987 El Niño. *Nature,* **351,** 27–32.

Raval, A., and V. Ramanathan, 1989: Observational determination of the greenhouse effect. *Nature,* **342,** 758–761.

Reynolds, R. W., and T. M. Smith, 1995: A high-resolution global sea surface temperature climatology. *J. Climate,* **8,** 1571–1583.

Salathe, E. P., and D. L. Hartmann, 1997: A trajectory analysis of tropical upper-tropospheric moisture and convection. *J. Climate,* **10,** 2533–2547.

Schneider, E. K., 1977: Axially symmetric steady-state models of the basic state for instability and climate studies. Part II: Nonlinear calculations. *J. Atmos. Sci.,* **34,** 280–296.

Schubert, W. H., P. E. Ciesielski, C. Lu, and R. H. Johnson, 1995: Dynamical adjustment of the trade wind inversion layer. *J. Atmos. Sci.,* **52,** 2941–2952.

Shine, K. P., and A. Sinha, 1991: Sensitivity of the Earth's climate to height-dependent changes in the water vapor mixing ratio. *Nature,* **354,** 382–384.

Sun, D.-Z., and R. S. Lindzen, 1993: Distribution of tropical tropospheric water vapor. *J. Atmos. Sci.,* **50,** 1643–1660.

——, and Z. Liu, 1996: Dynamic ocean–atmosphere coupling: A thermostat for the tropics. *Science,* **22,** 1148–1150.

Wallace, J. M., 1992: Effect of deep convection on the regulation of tropical sea surface temperature. *Nature,* **357,** 230–231.

Xu, K.-M. and K. A. Emanuel, 1989: Is the tropical atmosphere conditionally unstable? *Mon. Wea. Rev.,* **117,** 1471–1479.

Yang, H., and R. T. Pierrehumbert, 1994: Production of dry air by isentropic mixing. *J. Atmos. Sci.,* **51,** 3437–3454.

Zhang, G. J., and M. J. McPhaden, 1995: The relationship between sea surface temperature and latent heat flux in the equatorial Pacific. *J. Climate,* **8,** 589–605.